

Fig. 6. Distribution of the temperature coefficient.

The stability was measured by using 38 devices which were constructed using Philips MR 020 metal-film resistors and Evox polystyrene capacitors. Fig. 6 shows the distribution of the temperature coefficient of the pulsewidth.

#### ACKNOWLEDGMENT

The author wishes to thank Prof. P. Jääskeläinen for his interest and encouragement. He also wishes to thank Dipl. Eng. M. Salste for helpful suggestions.

#### REFERENCES

- [1] L. Strauss, *Wave Generation and Shaping*. New York: McGraw-Hill, 1970.
- [2] P. Lappalainen, "A method for regulating the temperature coefficient of a semiconductor diode," Helsinki Univ. Technology, Appl. Electron. Lab., Internal Rep. 3, 1970.
- [3] E. Heiber, "Über die Anwendungsmöglichkeiten von Korle- and Metallschichtwiderständen," *Elektronik*, vol. 11, no. 5, May 1962.
- [4] Fairchild Semiconductor, "Fairchild Semiconductor Integrated Circuit Data Catalog 1970."
- [5] P. Lappalainen, "A high performance monostable multivibrator," Helsinki Univ. Technology, Appl. Electron. Lab., Res. Rep. 10, 1971.

## A High Output Resistance Current Source

RICHARD C. JAEGER

**Abstract**—A current source based upon a pair of transistors in a cascode connection is discussed. The emitter-referenced cascode current source can offer as much as two orders of magnitude improvement in output resistance when compared to other current sources.

### I. INTRODUCTION

In order to obtain maximum common-mode input resistance and common-mode rejection ratio (CMRR) from differential amplifiers [1], a current source with an output resistance as high as possible is desirable. The current source of Fig. 1(d)

Manuscript received October 12, 1973; revised February 4, 1974.

The author was with the IBM Corporation, Boca Raton, Fla. He is now with the IBM Watson Research Center, Yorktown Heights, N. Y. 10598.

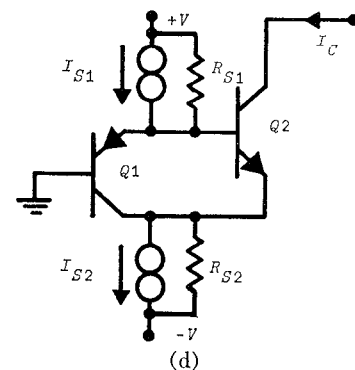
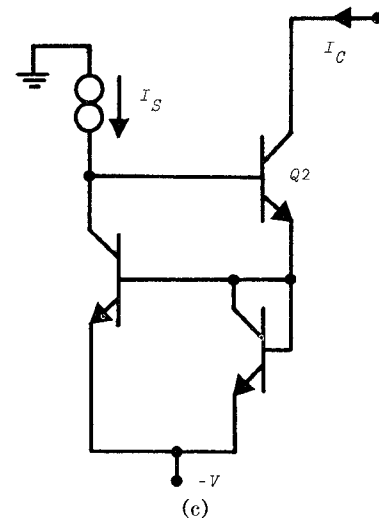
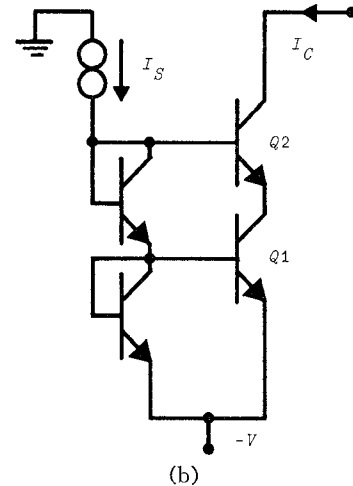
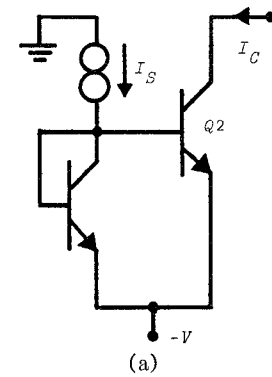


Fig. 1. (a) Current mirror. (b) Standard cascode source. (c) Wilson source. (d) Emitter-referenced cascode source.

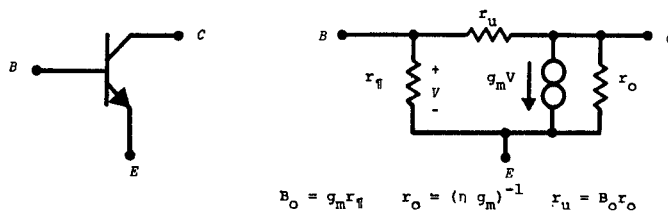


Fig. 2. Transistor pi-model.

TABLE I

Current Source	Output Conductance	Measured Output Resistance <sup>a</sup>
Current mirror	$g_{o2}$	130 k $\Omega$
Standard cascode source	$2g_{u2} + 2g_{o2}\eta_1 \frac{g_{m1}}{g_{m2}} + \frac{g_{o2}}{B_{o2}}$	—
Wilson source	$2g_{u2} + 2 \frac{g_{o2}}{B_{o2}}$	3.5 m $\Omega$
Emitter-referenced cascode source	$\frac{g_{o2}}{B_{o1}} \left( \frac{1}{B_{o2}} + \eta_1 \frac{g_{m1}}{g_{m2}} \right) + g_{u2} \left( \frac{1}{g_{m1}R_{S1}} + \frac{1}{B_{o1}} \right) + \eta_2 \left( g_{u1} + \frac{1}{R_{S2}} \right)$	60 m $\Omega$

<sup>a</sup>  $I_C = 1$  mA,  $I_{S2} = 2 I_{S1}$ ,  $B_{o2} = 240$ ,  $B_{o1} = 15$ .

can have an output resistance one to two orders of magnitude greater than that of conventional current sources.

## II. ANALYSIS

The output resistance of the current mirror of Fig. 1 is limited by the collector-emitter resistance of the output device Q2. The output resistance of the standard cascode and Wilson [2] current sources is limited by the collector-base resistance of the output device. A higher output resistance source is obtained using transistors in the emitter-referenced cascode configuration of Fig. 1. By referencing the base of the output device Q2 to the emitter potential of Q1 [3], a significant improvement in output resistance is obtained. A tedious but straightforward analysis of the current source output conductance using the pi-model of Fig. 2 results in the relationship below:

$$G_o = \frac{g_{o2}}{B_{o1}} \left( \frac{1}{B_{o2}} + \eta_1 \frac{g_{m1}}{g_{m2}} \right) + g_{u2} \left( \frac{1}{g_{m1}R_{S1}} + \frac{1}{B_{o1}} \right) + \eta_2 \left( g_{u1} + \frac{1}{R_{S2}} \right). \quad (1)$$

$R_{S1}$  = output resistance of  $I_{S1}$ .

$R_{S2}$  = output resistance of  $I_{S2}$ .

A comparison of the output conductances of the sources of Fig. 1 is given in Table I. The emitter-referenced cascode current source output resistance is improved by approximately a factor of  $B_o$  compared to the output resistance of either the standard cascode or Wilson current sources.

Examination of (1) yields the conditions necessary to obtain

the resistance level given in Table I. The output resistance  $R_{S2}$  of the bias source  $I_{S2}$  appears in parallel with  $g_{u1}$ . Therefore, the  $I_{S2}$  source should have an output resistance equivalent to that of the Wilson source.

The output resistance  $R_{S1}$  of the bias source  $I_{S1}$  should be large enough so that

$$g_{m1}R_{S1} > B_{o1}. \quad (2)$$

The requirement of (2) can be met with a source consisting of simply a resistor or a current mirror.

## III. PRACTICAL SOURCES

An emitter-referenced cascode current source with biasing networks is given in Fig. 3(a). Source  $I_{S1}$  is implemented using a current mirror.  $I_{S2}$  is a Wilson current source. The output resistance of this source approaches:

$$G_o \doteq 2 \frac{g_{u2}}{B_{o1}}.$$

As bipolar-JFET processing matures, the source of Fig. 3(b) will become quite attractive. This source requires a minimum of external bias elements, and can have a very high output resistance.

## IV. MEASUREMENTS AND CONCLUSION

Results of measurements of the output resistance of the current mirror, Wilson source, and emitter-referenced cascode source of Fig. 1 are presented in Table I. The sources were constructed using RCA CA-3096 devices. A 1-mA source current was chosen to facilitate the resistance measurements. The results verify that the emitter-referenced cascode current source

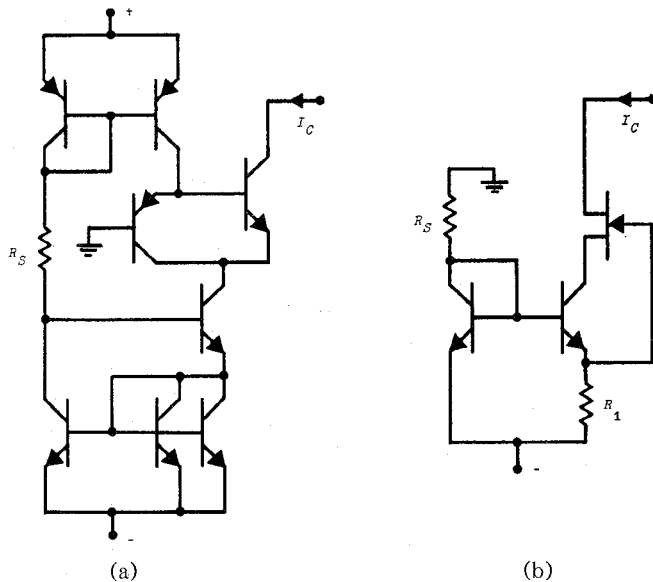


Fig. 3. Emitter-referenced cascode current sources.

offers a significant improvement in output resistance when compared to other sources.

#### REFERENCES

- [1] R. C. Jaeger and G. A. Hellwarth, "On the performance of the differential cascode amplifier," *IEEE J. Solid-State Circuits*, vol. SC-8, pp. 169-174, Apr. 1973.
- [2] G. R. Wilson, "A monolithic junction FET-*n-p-n* operational amplifier," *IEEE J. Solid-State Circuits*, vol. SC-3, pp. 341-348, Dec. 1968.
- [3] T. M. Frederiksen, "A monolithic high-power series voltage regulator," *IEEE J. Solid-State Circuits*, vol. SC-3, pp. 380-387, Dec. 1968.

## The Large Signal Input Capacitance of a Transistor Amplifier

R. R. DERYNCK AND R. H. JOHNSTON

**Abstract**—A simple bipolar transistor amplifier generates subharmonics at frequencies well below  $f_\beta$ . A study of the results of a computer-aided design program reveals that a large nonlinear capacitance appears at the transistor input. The source of the nonlinear capacitance is found.

#### INTRODUCTION

A simple bipolar transistor amplifier can generate subharmonics at both high and low frequencies when driven by a sinusoid [1]. High-frequency subharmonic generation is due chiefly to the nonlinear diffusion capacitance of the tran-

Manuscript received November 1, 1973; revised February 22, 1974.

R. R. Derynck was with the Department of Electrical Engineering, University of Calgary, Calgary, Alta., Canada. He is now with Hudson's Bay Oil and Gas Company, Ltd., Calgary, Alta., Canada.

R. H. Johnston is with the Department of Electrical Engineering, University of Calgary, Calgary, Alta., Canada.

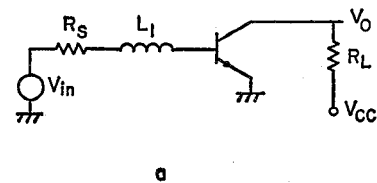


Fig. 1. The transistor amplifier circuit simulated using SCEPTRE which generated subharmonics.

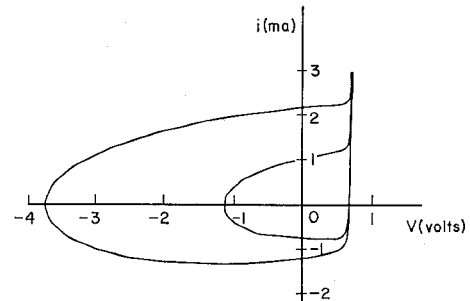


Fig. 2. The current-voltage plot of the intrinsic base. The fundamental frequency is 800 kHz, the subharmonic frequency is 400 kHz.

sistor. Low-frequency ( $f \ll f_\beta$ ) subharmonic generation cannot be attributed to the diffusion capacitance owing to its negligible influence on the device currents. The subharmonic must be generated by either a nonlinear capacitance or a nonlinear negative resistance [2]. At low frequencies the transistor does not appear to have a large nonlinear capacitance or a negative resistance. It is therefore desirable to determine exactly how the subharmonic is generated in the transistor.

#### TRANSISTOR MODELING

A SCEPTRE [3] circuit analysis program is used to simulate the transistor circuit shown in Fig. 1. The standard SCEPTRE transistor model is used neglecting the diffusion capacitance. In addition, the depletion layer capacitances are assumed to be linear. The program accurately predicts the presence of a subharmonic and the calculated transistor current and voltage waveforms correspond closely to those observed in the actual circuit [1].

From the SCEPTRE program, the current flowing into the intrinsic base of the transistor is plotted as a function of the voltage at that point. See Fig. 2. The generated subharmonic causes two distinct loops to appear in the  $i-v$  plot. Each loop of the plot is similar to the  $i-v$  characteristic of a capacitor and a diode in parallel.

Because of this similarity, it is assumed that the intrinsic base input acts as a nonlinear  $RC$  network to ground. See Fig. 3(a). Both the conductance and the capacitance are assumed to be voltage dependent. The current in this circuit is

$$i_b = C(v_{b'e}) \frac{dv_{b'e}}{dt} + i_g(v_{b'e}) \quad (1)$$

where  $C(v_{b'e})$  and  $i_g(v_{b'e})$  are defined for any value of  $v_{b'e}$ .  $v_{b'e}$  is the intrinsic base to emitter voltage

$$v_{b'e} = i_b r_{b'b} + v_{b'e}$$

However  $dv_{b'e}/dt$  depends on the drive voltage. During steady-state operation there are at least two values of  $dv_{b'e}/dt$  associated with each value of  $v_{b'e}$ . It is therefore possible to write: